Journal of Colloid and Interface Science 325 (2008) 419–424

Contents lists available at ScienceDirect

Journal of Colloid and Interface Science

www.elsevier.com/locate/jcis

Solution decomposition of the layered double hydroxide of Co with Fe: Phase segregation of normal and inverse spinels

Sylvia Britto [a], P. Vishnu Kamath [a,*], N. Ravishankar [b]

[a] Department of Chemistry, Central College, Bangalore University, Bangalore 560 001, India
[b] Materials Research Centre, Indian Institute of Science, Bangalore 560 012, India

ARTICLE INFO

Article history:
Received 25 March 2008
Accepted 21 May 2008
Available online 28 May 2008

Keywords:
Layered double hydroxides
Solution decomposition
Inverse spinel

ABSTRACT

The nitrate-intercalated layered double hydroxide of Co with Fe decomposes on hydrothermal treatment to yield an oxide residue at a temperature as low as 180 °C. The oxide product is phase segregated into a Co_3O_4-type normal spinel and a $CoFe_2O_4$-type inverse spinel. Phase segregation is facilitated as decomposition in a solution medium takes place by dissolution of the precursor hydroxide followed by reprecipitation of the oxide phases. In contrast, thermal decomposition takes place at 400 °C. This temperature is inadequate to induce diffusion in the solid state whereby phase segregation into the thermodynamically stable individual spinels is suppressed. The result is a single-phase metastable mixed spinel oxide. This is rather uncommon in that a hydrothermal treatment yields thermodynamically stable products where as thermal decomposition yields a metastable product.

1. Introduction

Layered double hydroxides (LDHs) having the formula, $[M^{II}_{1-x}M'^{III}_x(OH)_2][A^{n-}]_{x/n}\cdot yH_2O$ ($0.2 \leqslant x \leqslant 0.33$) are well known precursors for the synthesis of transition metal oxides [1–5] as they have a low decomposition temperature. Further, the decomposition is accompanied by a large mass loss, by virtue of which, the product oxide has a nanoparticulate morphology [1]. There is an added significance, in the case of Co(II)-based LDHs, as the product of decomposition is a spinel [1,3–6]. Spinels of Co^{2+} (general formula, CoB_2O_4) are technologically important as magnetic storage materials and catalysts [7–9].

The unitary hydroxide of Co(II), $Co(OH)_2$, decomposes at 220 °C to yield Co_3O_4 ($B = Co^{3+}$). Co_3O_4 is a normal spinel. The LDHs of Co^{2+} with trivalent cations, M'^{3+}, yield the mixed spinel $Co(Co, M'^{3+})O_4$. When $M' = Al$ or Cr, the product is a normal spinel. But interesting possibilities arise when the trivalent cation is Fe^{3+}, as cobalt ferrite, $CoFe_2O_4$, is an inverse spinel owing to the poor octahedral crystal field stabilization energy of Fe^{3+}.

Consequently when the LDH of Co with Fe having the formula $[Co_2Fe(OH)_6]$ $(NO_3)\cdot yH_2O$ ($x = 0.33$) is decomposed, there are many possibilities: (a) the oxide product could be a single-phase mixed spinel of the type $Co^{2+}(Co^{3+}, Fe^{3+})O_4$ or (b) the oxide may phase segregate into a normal spinel, Co_3O_4 and an inverse spinel, $CoFe_2O_4$.

The thermal decomposition of the Co–Fe LDHs has been reported over a range of temperatures. At lower temperatures (<450 °C) a single-phase Fe-substituted Co-rich spinel [4,6] is observed. The Fe–Co–O phase diagram [10,11] shows that for Co/(Co + Fe) ratios corresponding to that found in LDHs (0.66–0.80), complete solubility of Co and Fe spinels is attained only above ~900 °C. At lower temperatures (<900 °C), a solubility gap is seen in the phase diagram comprising cobaltite and ferrite. The single-phase spinels obtained at still lower temperatures (<450 °C) are therefore metastable.

Another method of decomposing a LDH is by hydrothermal treatment. Hydrothermal treatment is generally employed to promote crystal growth [12] or achieve a gel to crystallite conversion [13]. In an LDH, all the cations occupy octahedral sites. LDHs comprising cations with low octahedral crystal field stabilization energies such as Zn^{2+}, Co^{2+}, and Fe^{3+} have poor stability. Such LDHs decompose on hydrothermal treatment [14,15]. Since hydrothermal transformations take place within a solution medium, we refer to such a decomposition reaction as solution decomposition.

In this paper we report the solution decomposition of the Co–Fe LDH and compare the oxide products obtained with those obtained from thermal decomposition.

2. Materials and methods

The Co–Fe LDHs were prepared by coprecipitation by the addition of a mixed metal ($Co^{2+} + Fe^{3+}$) nitrate solution (total concentration, 0.5 M; $[Co^{2+}]/[Fe^{3+}] = 2.0, 3.0$) to a solution containing three times the stoichiometric excess of the required anion (NO_3^-

* Corresponding author. Fax: +91 80 22961354.
E-mail address: vishnukamath8@hotmail.com (P.V. Kamath).

0021-9797/$ – see front matter
doi:10.1016/j.jcis.2008.05.041

or CO_3^{2-}) taken as its sodium salt. The reaction was carried out at constant pH 7 using a Metrohm Model 718 Stat Titrino operating in the STAT mode under constant stirring ($T = 65\,^{\circ}C$). N_2 gas was bubbled through the reaction mixture during the preparation of the Co–Fe–NO_3 LDH. All the products were washed by centrifugation with decarbonated, deionized (Millipore ELIX3 ion exchanger) water and dried in an air oven at 65 °C.

Both the carbonate and nitrate LDHs were hydrothermally treated ($T = 150$–$180\,^{\circ}C$, 24 h) under autogenous pressure (50% filling) using a Teflon-lined autoclave (volume, 80 ml; 0.4 g LDH dispersed in 40 ml of water). In separate experiments, the LDHs were also calcined in a muffle furnace at 400 and 600 °C for 18 h each in separate experiments.

Powder diffraction data were collected on a Bruker D8 Advance powder X-ray diffractometer (Cu$K\alpha$ radiation, $\lambda = 1.5418$ Å) fitted with a bent crystal graphite secondary monochromator. Data were collected at a continuous scan rate of 0.5° 2θ min^{-1} and rebinned into steps of 0.02° 2θ. PXRD profiles of the oxide residue were fit by the Rietveld method using the Fullprof suite with either a single Co_3O_4-type structure model or with two structure models (one normal and the other inverse spinel). TG data were obtained using a Mettler Toledo TGA/SDTA Model 851^e system after equilibrating the sample at 100 °C (30 min) and then ramping the temperature up (100–800 °C, heating rate 5 °C min^{-1}) in air. Transmission electron microscopy was (TEM) was carried out using a JEOL 200CX microscope operated at 160 kV. Powdered samples were dispersed on carbon-coated grids.

3. Results

In Fig. 1 is shown the PXRD pattern of Co_3Fe–NO_3 LDH. The pattern can be indexed on the basis of a hexagonal cell ($a = 3.13$ Å, $c = 23.8$ Å) and exhibits three classes of reflections characteristic of the LDHs. The set of low angle reflections, 00ℓ, can be used to identify the nature of the interlayer anion. The basal spacing ($d_{003} = 7.9$ Å) agrees with what is expected of the nitrate present in D_{3h} orientation with the 3-fold axis being parallel to the c-direction. The set of high angle (50–60° 2θ) reflections is characteristic of the metal–metal distances within the interlayer. In addition, a set of mid-2θ reflections is observed. The non-uniform broadening of these reflections indicates a turbostratically disordered material.

Hydrothermal treatment of this sample was originally carried out with the objective of bringing about structural order. However, turbostratic disorder could not be eliminated up to 150 °C. At 180 °C however, the LDH was found to decompose to yield a Co_3O_4-type spinel as indicated by the PXRD pattern shown in Fig. 2. While all observed peak positions match with those expected of a Co_3O_4-type spinel, the peaks corresponding to different reflections exhibit an asymmetry on the low angle side. The asym-

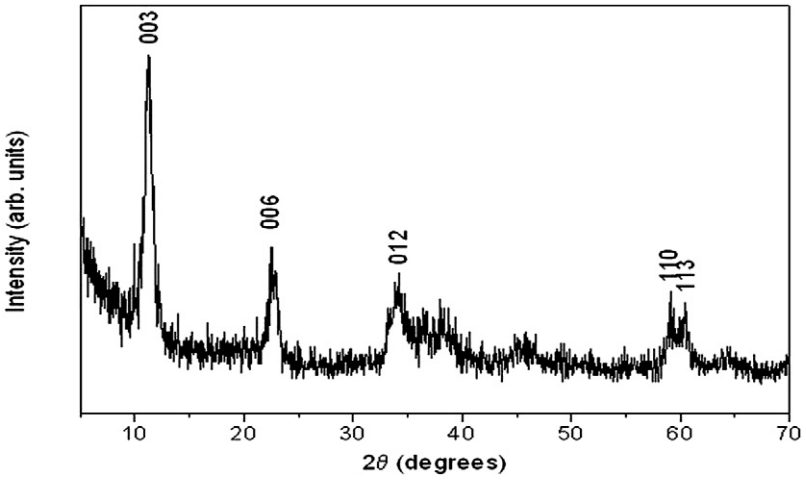

Fig. 1. PXRD pattern of the Co_3Fe–NO_3 LDH.

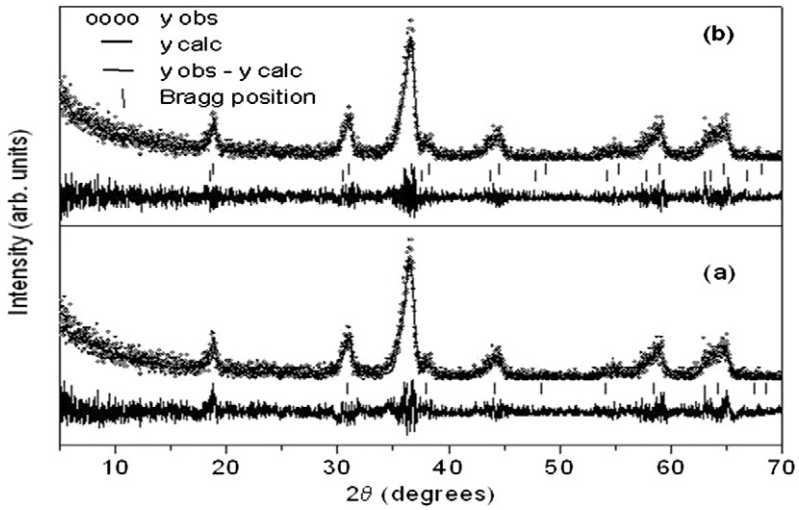

Fig. 2. Rietveld fits of the observed PXRD profile of the oxide residue obtained from the solution decomposition of the Co_3Fe–NO_3 LDH using (a) one phase structure model, (b) using two structure models.

Table 1

Sample	R_p	R_{wp}	R_{exp}	χ^2	Bragg R-factor	
					$Co_{3-x}Fe_xO_4$	$CoFe_2O_4$
Co_3Fe–NO_3HT 180 °C, Fig. 2a, single-phase with asymmetry factor	55.2	52.7	46.93	1.26	13.3	
Co_3Fe–NO_3HT 180 °C, Fig. 2b (two-phase)	46.9	47.4	44.32	1.14	8.65	13.00
Co_3Fe–NO_3D 400 °C, Fig. 6a	50.5	49.7	48.5	1.05	9.23	
Co_2Fe–NO_3 D 400 °C, Fig. 6b	59.3	59.9	56.09	1.14	15.38	

HT: hydrothermally decomposed; D: thermally decomposed.

metry is greater in peaks appearing at high angles. In order to analyze the source of this asymmetry, the pattern was analyzed by Rietveld refinement. The asymmetry in the observed peaks could be either due to instrumental factors (axial divergence of the incident beam) or the presence of a structurally related second phase. If the asymmetry is due to instrumental factors, then it should increase at decreasing angles [16], but in our pattern the opposite trend is observed. Nevertheless, both these possibilities were explored.

The observed profile was used to refine a Co_3O_4-like structure by the Rietveld method and the results are shown in Fig. 2a. The goodness-of-fit parameters are given in Table 1. These are higher than normally accepted values owing to the poor crystallinity of the samples. The asymmetry in the peak shape was fitted by incorporating an asymmetry parameter and then refining it. This fit corresponds to a single-phase structure model, $Co_{3-x}Fe_xO_4$. Alternatively, the observed profile was fit to a two-phase mixture comprising the normal spinel Co_3O_4 (ICSD No: 24210) and the inverse spinel $CoFe_2O_4$ (ICSD No: 98553). The Bragg reflections of these two phases are progressively separated at higher angles and account for the asymmetry of the observed peak shapes without the incorporation of the asymmetry parameter in the profile function. The results of the Rietveld fit are shown in Fig. 2b and the refined parameters are shown in Table 1. It is evident from an examination of the R values that the two-phase fit is superior to the single-phase fit. According to Young [16], more important than the R-values is an examination of the difference profile. It is clear that the difference profile in Fig. 2a has systematic residual intensities at 18–20° 2θ and ∼65° 2θ. These are eliminated in Fig. 2b, showing a two-phase model fits the observed data better.

In order to further examine the phenomenon of phase segregation into normal and inverse spinels under hydrothermal conditions, it was thought that a sample with higher iron content would lead to a greater degree of phase segregation. The PXRD pattern of Co_2Fe–NO_3 LDH is shown in Fig. 3a. While the poor crystallinity of the sample does not permit accurate comparison of a-parameter, a comparison of the TGA data of the two LDHs, discussed in the next section, points to the formation of an LDH with a higher iron content.

Hydrothermal treatment of this sample at 180 °C also leads to decomposition of the LDH. In this pattern (see Fig. 3b), the splitting of the peaks in the high angle region is better resolved indicating greater phase segregation due to the higher iron content in the precursors. The reflections towards the higher angle side are due to Co_3O_4 and those to the lower angle side are due to $CoFe_2O_4$.

The PXRD pattern of Co_3Fe–CO_3 LDH is shown in Fig. 4a. The d-spacing of the 003 reflection, 7.59 Å, corresponds to a carbonate-intercalated LDH. The relative sharpness of the reflections in the mid-2θ region indicates a better ordered material when compared to the nitrate LDH. It is seen that upon hydrothermal treatment, all the reflections corresponding to the LDH have disappeared indicating a break down of the LDH structure (see Fig. 4b). The pattern can be indexed to a mixture of β-$Co(OH)_2$ and γ-Fe_2O_3.

The products obtained by solution decomposition were compared with those obtained after calcination at 400 °C. TG–DTG data of the precursor LDHs are shown in Fig. 5. The single step weight loss observed in both the carbonate and nitrate LDHs point to simultaneous dehydration and dehydroxylation. The DTG curve indicates that the CO_3-LDH decomposes at 167 °C (Fig. 5a) while the NO_3-LDH decomposes at a slightly higher temperature at 185 °C (Fig. 5b). Further, the Co_2Fe–NO_3 LDH (Fig. 5c) decomposes at a slightly lower temperature (175 °C) when compared with the Co_3Fe–NO_3 LDH (185 °C). This is due to the higher iron content in this sample. The Co_2Fe–NO_3 LDH exhibits a total mass loss of 32.5% giving a nominal formula $[Co_{0.66}Fe_{0.33}(OH)_2](NO_3)_{0.33}\cdot 0.25H_2O$ while the 3:1 LDH exhibits a mass loss of 30.2% from which the nominal formula of this LDH was calculated to be $[Co_{0.75}Fe_{0.25}(OH)_2](NO_3)_{0.25}\cdot 0.25H_2O$.

On calcination at 400 °C, Co_3Fe–NO_3 LDH decomposes to give a Co_3O_4-type spinel. The peaks due to the various reflections are symmetrically broadened. A Rietveld fit of this pattern was done using the $Co_{3-x}Fe_xO_4$ structure model (Fig. 6a). While the poor

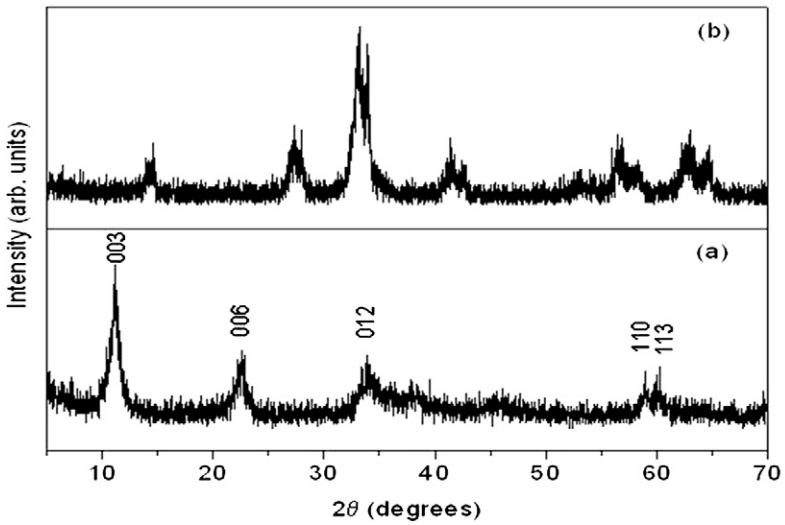

Fig. 3. (a) PXRD pattern of the Co_2Fe–NO_3 LDH. (b) PXRD pattern of the oxide obtained by the solution decomposition of (a).

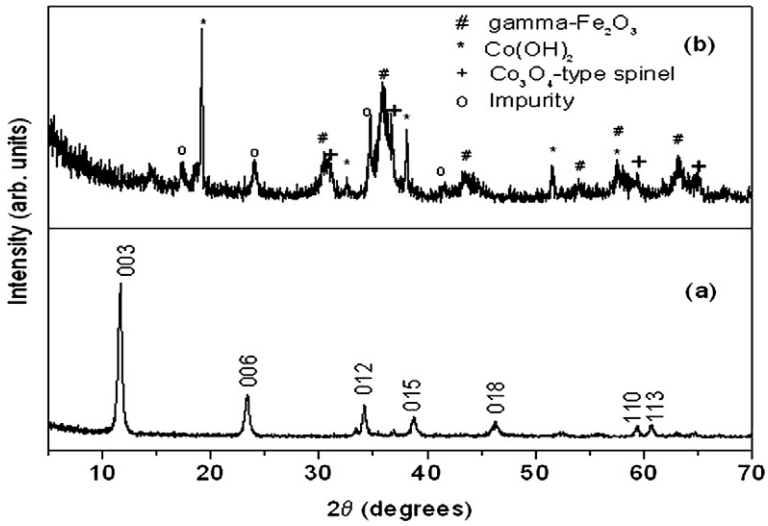

Fig. 4. (a) PXRD pattern of the $Co_3Fe–CO_3$ LDH. (b) PXRD pattern of the solid obtained by the solution decomposition of (a).

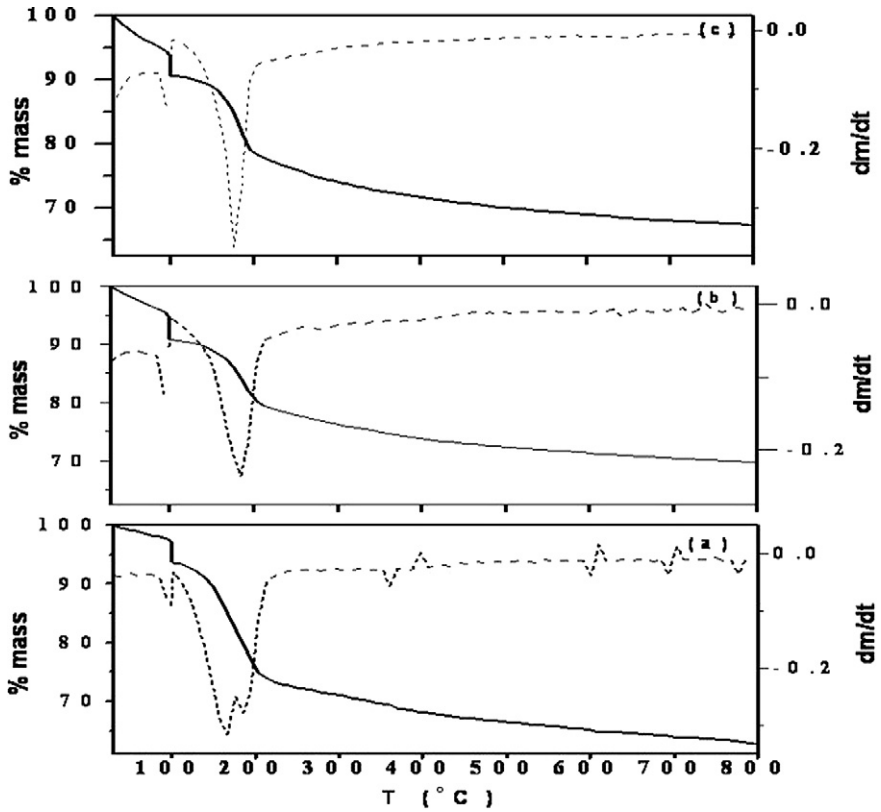

Fig. 5. (a) TG–DTG curve of (a) $Co_3Fe–CO_3$ LDH, (b) $Co_3Fe–NO_3$ LDH, (c) $Co_2Fe–NO_3$ LDH.

crystallinity of this sample implies that the cation distribution obtained by the Rietveld technique cannot be relied upon, an examination of the *a*-parameter gives an indication of the site occupied by Fe^{3+}. Pure Co_3O_4 has a lattice parameter of 8.08 Å. In comparison, the *a*-parameter of this spinel is found to be 8.14 Å. The higher *a*-parameter is indicative of Fe^{3+} (O_h ionic radius = 0.77 Å) substituting a part of the Co^{3+} (ionic radius = 0.68 Å) in the octahedral sites. In comparison, the single phase spinel obtained on decomposition of $Co_2Fe–NO_3$ (Fig. 6b) exhibits a slightly larger *a*-parameter of 8.16 Å in concordance with the higher Fe^{3+} content from the precursor.

The carbonate LDH is also seen to decompose to give a single-phase Co_3O_4-type spinel on calcination at 400 °C (data not given). In this case also, the higher *a*-parameter of 8.17 Å indicates a spinel in which Fe^{3+} ions substitute a part of the Co^{3+} ions in the octahedral sites of Co_3O_4.

Fig. 7A shows a selected area electron diffraction pattern from the oxide residue obtained by thermal decomposition of $Co_3Fe–NO_3$ LDH. The pattern can be indexed to a Co_3O_4-type phase. The diffuse rings indicate the nanocrystalline nature of the sample. The SAED pattern of the hydrothermally treated sample is shown in Fig. 7B. Distinct splitting of the rings in the radial direction can be seen (as shown by arrows) indicating that two phases with close *d*-spacings could be present. This is consistent with the powder X-ray data that shows the presence of the Co_3O_4 type phase and the $CoFe_2O_4$ type phase in these samples.

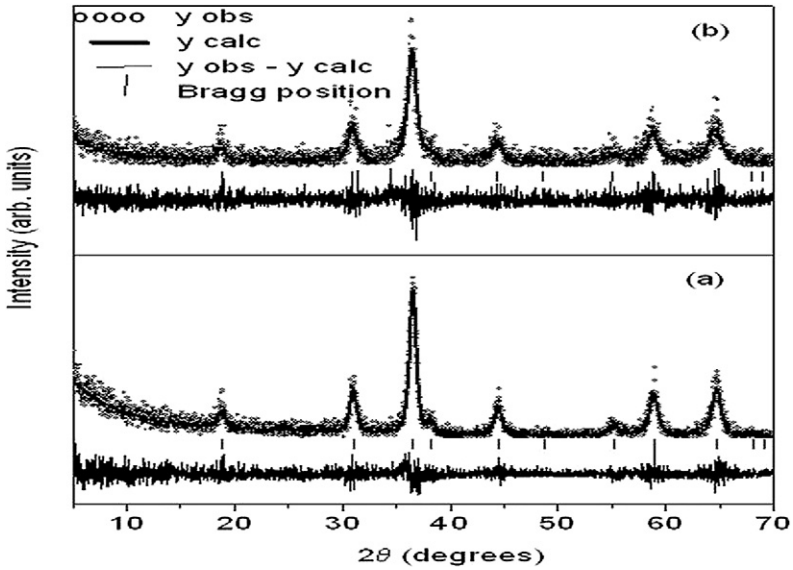

Fig. 6. Rietveld fits of the observed PXRD profile of the oxide residue obtained from the thermal decomposition at 400 °C of the (a) Co_3Fe–NO_3 LDH, (b) Co_2Fe–NO_3 LDH.

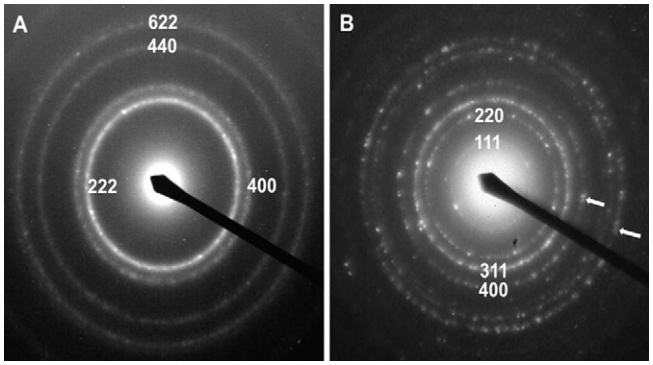

Fig. 7. SAED pattern of oxide reside obtained upon (a) thermal decomposition of Co_3Fe–NO_3 LDH, (b) solution decomposition of Co_3Fe–NO_3 LDH.

4. Discussion

As the LDH composition is divalent cation rich, $x = 0.25$–0.33, formation of a stoichiometric spinel requires that a part of the divalent cations be oxidized. In the case of the oxide product derived from the Co_3Fe-LDH, such an oxidation would lead to a spinel of the formula $Co^{II}Co^{III}_{1.26}Fe^{III}_{0.75}O_4$. In a spinel of this composition, it is expected that Co(III) would occupy octahedral sites due to its very high octahedral crystal field stabilization energy. There are then two possible cation distributions that the spinel can adopt: (i) The Fe(III) can occupy tetrahedral sites pushing Co(II) into octahedral sites giving a partly inverse spinel, (ii) Fe(III) can occupy octahedral sites along with Co(III) giving a primarily normal spinel in which Co(II) ions occupy tetrahedral sites. These two cation distributions are represented as shown below:

$$(Co^{II})\left[Co^{III}_{1.26},\ Fe^{III}_{0.75}\right]O_4, \tag{1}$$

$$\left(Fe^{III}_{0.75},\ Co^{II}_{0.21}\right)\left[Co^{III}_{1.26},\ Co^{II}_{0.78}\right]O_4, \tag{2}$$

where round brackets denote tetrahedral sites and square brackets denote octahedral sites.

Experimental results suggest that on thermal decomposition, the Co–Fe LDHs, yield a single-phase spinel having a cation distribution similar to (1) above. Navrotsky and co-workers [17] have shown that in an oxide of the spinel structure, Fe(III) has a 'definite' tetrahedral site preference. Therefore a spinel of the above composition is understandably metastable [10] and phase segregation into a cobalt rich normal spinel and iron rich inverse spinel is observed to occur at higher temperatures [6]. As both the single-phase spinel and the two-phase spinel have the same crystal structure, the formation of one product over the other would be dependent upon the site preference energies of the cations involved. In the LDH structure, Fe(III) occupies octahedral sites whereas Co(II) can occupy either octahedral sites as in β-$Co(OH)_2$ and Co-M(III)-LDHs or tetrahedral sites as in α-$Co(OH)_2$ [18]. It is observed that the metastable single-phase spinel is formed only on thermal decomposition. The formation of the single-phase spinel would require only diffusion of Co(II) ions from octahedral to tetrahedral sites while Fe(III) and Co(III) remain in octahedral sites. Phase segregation to a normal and inverse spinel on the other hand would require both migration of Co(II) into tetrahedral sites to give cobalt-rich spinel as well as migration of Fe(III) into tetrahedral sites to yield an iron rich spinel.

Therefore under conditions of solid state decomposition, where diffusion plays a large role, formation of the metastable single-phase spinel would be kinetically favoured over formation of the two-phase product.

Under hydrothermal conditions however, solubility would rule out any topochemical pathway for the decomposition and the thermodynamically stable phase segregated products would be energetically favoured. This is observed in the case of hydrothermal decomposition of Co_3Fe-nitrate LDH. Another possible factor driving phase segregation under hydrothermal conditions could be incomplete oxidation of Co(II) ions in the depleted oxidative atmosphere prevailing under hydrothermal conditions.

The overriding role played by solubility is further demonstrated by the decomposition of Co_3Fe–CO_3 LDH. It is known that carbonate LDHs are in general more stable than nitrate LDHs [19] and under hydrothermal conditions, this is reflected by the lower solubility of carbonate LDHs when compared with the nitrate LDHs. Decomposition of the carbonate LDHs under hydrothermal conditions is therefore not complete and β-$Co(OH)_2$ and γ-Fe_2O_3 are seen to have formed.

5. Summary

Decomposition of the Co–Fe LDH is seen to be kinetically controlled under thermal conditions leading to a single-phase metastable spinel. Under hydrothermal conditions however, de-

composition is seen to take place under thermodynamic control and is demonstrated by (1) formation of thermodynamically stable normal and inverse spinels and (2) the observation that the nitrate LDH leads to complete decomposition whereas the higher stability of carbonate-LDH leads to incomplete decomposition and formation of β-$Co(OH)_2$ and γ-Fe_2O_3.

Acknowledgments

The authors thank the Department of Science and Technology (DST), Government of India (GOI) for financial support. S.B. thanks the University Grants Commission, GOI for the award of a Senior Research Fellowship (NET). P.V.K. is a recipient of the Ramanna Fellowship of the DST.

References

[1] E.L. Uzunova, J.G. Mitov, D.G. Klissurski, Bull. Chem. Soc. Jpn. 70 (1997) 1985.
[2] F. Li, J. Liu, D.G. Evans, X. Duan, Chem. Mater. 16 (2004) 1597.
[3] E.L. Uzunova, D. Klissurski, I. Mitov, P. Stefanov, Chem. Mater. 5 (1993) 576.
[4] T. Baird, K.C. Campbell, P.J. Holliman, R. Hoyle, G. Noble, D. Stirling, B.P. Williams, J. Mater. Chem. 13 (2003) 2341.
[5] M.E.P. Bernal, R.J.R. Casero, V. Rives, Ceramics—Silikaty 48 (2004) 145.
[6] M. del Arco, R. Trujillano, V. Rives, J. Mater. Chem. 8 (1998) 761.
[7] R.R. Rajaram, P.A. Sermon, J. Chem. Soc. Faraday Trans. 81 (1985) 2577.
[8] R.R. Rajaram, P.A. Sermon, J. Chem. Soc. Faraday Trans. 81 (1985) 2593.
[9] Q. Song, Z.J. Zhang, J. Am. Chem. Soc. 126 (2004) 6164.
[10] M.M.J. Robin, J. Benard, Comptes Rendus 232 (1951) 1830.
[11] I.-H. Jung, S.A. Decterov, A.D. Pelton, H.-M. Kim, Y.-B. Kang, Acta Mater. 52 (2004) 507.
[12] L. Hickey, J.T. Kloprogge, R.L. Frost, J. Mater. Sci. 35 (2000) 4347.
[13] M. Nayak, T.R.N. Kutty, V. Jayaraman, G. Periaswamy, J. Mater. Chem. 7 (1997) 2131.
[14] S. Britto, A.V. Radha, N. Ravishankar, P.V. Kamath, Solid State Sci. 9 (2007) 279.
[15] M.A. Ulibarri, J.M. Fernandez, F.M. Labajos, V. Rives, Chem. Mater. 3 (1991) 626.
[16] R.A. Young (Ed.), The Rietveld Method, Oxford Univ. Press, New York, 1993.
[17] A. Navrotsky, O.J. Kleppa, J. Inorg. Nucl. Chem. 29 (1967) 2701.
[18] R. Ma, Z. Liu, K. Takada, K. Fukuda, Y. Ebina, Y. Bando, T. Sasaki, Inorg. Chem. 45 (2006) 3964.
[19] R.K. Allada, A. Navrotsky, H.T. Berbeco, W.H. Casey, Science 296 (2002) 721.